

Quantum-Dense Metrology

Sebastian Steinlechner, Jöran Bauchrowitz, Melanie Meinders,

Helge Müller-Ebhardt, Karsten Danzmann, and Roman Schnabel

Institut für Gravitationsphysik, Leibniz Universität Hannover and Max-Planck-Institut für Gravitationsphysik (Albert-Einstein-Institut), Callinstr. 38, 30167 Hannover, Germany

(Dated: July 17, 2018)

Quantum metrology utilizes entanglement for improving the sensitivity of measurements [1, 2]. Up to now the focus has been on the measurement of just *one* out of two non-commuting observables. Here we demonstrate a laser interferometer that provides information about *two* non-commuting observables, with uncertainties below that of the meter's quantum ground state. Our experiment is a proof-of-principle of quantum dense metrology, and uses the additional information to distinguish between the actual phase signal and a parasitic signal due to scattered and frequency shifted photons. Our approach can be readily applied to improve squeezed-light enhanced gravitational-wave detectors at *non*-quantum noise limited detection frequencies in terms of a sub shot-noise veto-channel.

Heisenberg's uncertainty principle states that it is generally not possible to gather precise information about non-commuting observables of a physical system. Prominent examples are the position and the momentum of a particle or the amplitude and phase quadratures of an electro-magnetic wave. In this way the uncertainty of meter systems, e.g. laser light, limits the sensitivity in metrology, even if the quantum mechanical uncertainty of the measurement object itself can be neglected. Using a meter system in a nonclassical state it is, nevertheless, possible to measure one observable with arbitrarily high precision. If its imprecision is 'squeezed' below the zero-point fluctuation of the meter system the regime of quantum metrology is reached, as demonstrated in proof-of-principle experiments [3–10]. Recently, quantum metrology was applied to an operating gravitational wave detector [11].

For a wide application of quantum metrology a rather general problem exists. In order to improve classical state-of-the-art measurement sensitivities, the concept of quantum metrology must be combined with state-of-the-art intense meter states. Current gravitational wave detectors, be they squeezed-light enhanced or not, use light fluxes of about 10^{20} photons per second [12]. Unfortunately, the scattering of just a single photon from the meter into the signal band per second and Hertz produces a significant parasitic signal against which quantum-noise squeezing is bootless. The scatter problem is understood as a *parasitic interference*, where vibrating scatter surfaces frequency-shift a tiny amount of photons into the detection band [13]. It is a well-known problem in high-precision laser interferometry [14–16]. We conjecture that the limitation of quantum metrology at lower detection frequencies as observed in [11] at least partially originates from parasitic interferences. In the future, even higher photon fluxes will be used [17], and parasitic interferences will become increasingly severe.

Here we propose *quantum-dense metrology* (QDM) to widen the application of quantum metrology into the

regime where parasitic interferences are a limiting noise source. We present a proof of principle experiment that discriminates between the actual science signal and a parasitic interference with sub-shot-noise measurement precision, exploiting the generally different phase space orientation of the two. It is shown that QDM provides a non-classical veto-channel during signal searches and is thus able to improve a non-classical interferometer beyond what is possible with conventional quantum metrology.

Our readout scheme is based on Einstein-Podolsky-Rosen entanglement [18], which has been first considered for metrology by D'Ariano *et al.* [19]. Following this work we replace the single meter state by a bipartite, two-mode-squeezed entangled state, as depicted in Fig. 1. One mode of the entangled system serves as the new meter state, whereas the other mode is kept as an external reference for the measurement device. Since the difference in position and the sum in momentum commute, $[\hat{x}_A - \hat{x}_B, \hat{p}_A + \hat{p}_B] = 0$, it is in principle possible to exactly measure the distance in phase space between the two modes. Thus we overcome the limitation that is set by the Heisenberg Uncertainty Relation for reading out two orthogonal quadratures of a *single* system by performing all measurements in relation to the reference beam. Such measurements have previously also been considered for super-dense coding with the purpose of doubling the capacity of quantum communication channels [20, 21]. The required continuous-variable entangled states were experimentally pioneered by Ou *et al.* [22], see also [23–25] for more recent experiments. In contrast to all previous proposals, QDM as introduced here uses two-mode squeezing of *non*-orthogonal quadratures. We show that this opens a way to optimize the science signal-to-noise ratio.

The measurement problem of reading out two orthogonal quadratures was pioneered by Arthurs and Kelly [26]. For a light field whose (classical) signal is given by a displacement projected onto the quadratures $X(t) = \langle \hat{x}(t) \rangle$

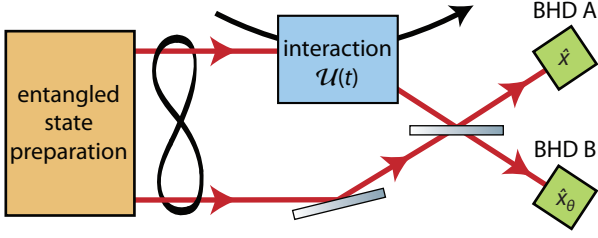


FIG. 1. Schematic showing the underlying principle of quantum-dense metrology. The meter system consists of a bipartite continuous-variable entangled state, of which one part interrogates the system of interest in an interaction zone, while the other part is kept as a local reference. Both entangled modes are recombined after the interaction, and each output is detected via a balanced homodyne detector (BHD).

and $P(t) = \langle \hat{p}(t) \rangle$, the signal-normalized Heisenberg uncertainty relation reads

$$\frac{\Delta^2 \hat{x}(t) \Delta^2 \hat{p}(t)}{|X(t)|^2 |P(t)|^2} \geq \frac{1}{4|X(t)|^2 |P(t)|^2}, \quad (1)$$

where the quadrature variances for the ground state are normalized to $\Delta^2 \hat{x}(t) = \Delta^2 \hat{p}(t) = 1/2$. However, actually measuring both quadratures simultaneously (subscript ‘sim’) with e.g. an eight-port homodyne detector [27] leads to an uncertainty relation that is four times as large [26],

$$\frac{\Delta^2 \hat{x}_{\text{sim}}(t) \Delta^2 \hat{p}_{\text{sim}}(t)}{|X_{\text{sim}}(t)|^2 |P_{\text{sim}}(t)|^2} \geq \frac{1}{|X(t)|^2 |P(t)|^2}. \quad (2)$$

With QDM as presented here, the simultaneous readout is no longer limited by such an uncertainty relation. Instead, the achievable sensitivity is directly connected to the squeezing parameters r_a , r_b of the initial squeezed beams. Entangling those beams with relative angle θ allows for a simultaneous detection of the quadrature \hat{x} and the rotated quadrature $\hat{x}_\theta = \hat{x} \cos \theta + \hat{p} \sin \theta$ with

$$\frac{\Delta^2 \hat{x}_{\text{sim}}^{\text{ent}}(t) \Delta^2 \hat{x}_{\theta, \text{sim}}^{\text{ent}}(t)}{|X_{\text{sim}}^{\text{ent}}(t)|^2 |X_{\theta, \text{sim}}^{\text{ent}}(t)|^2} \geq \frac{e^{-2r_a} e^{-2r_b}}{|X(t)|^2 |X_\theta(t)|^2}. \quad (3)$$

Setting $\theta = \pi/2$ the substantial improvement compared to the lower bound in inequality (2) becomes obvious. The Heisenberg uncertainty relation for a conventional readout based on a single-mode meter system (1) is surpassed for two-mode squeezing with $r > 0.3466$. In principle, QDM allows for a readout with arbitrary precision, in the limit of infinite squeezing. A detailed derivation of the above results can be found in the supplementary materials.

We proved the principle of quantum-dense metrology and its high potential for improving state-of-the-art laser interferometers in the following table-top experiment. In a Michelson-type laser interferometer (Fig. 2) with

arm lengths of about 7.5 cm we generated two signals in the megahertz regime. The actual interferometer phase signal was produced by modulating the PZT mounted north-arm mirror at 5.55 MHz. We intentionally introduced a parasitic signal at 5.17 MHz by PZT-modulating a small amount of light that leaked through the east-arm mirror. By adjusting the phase with which the light was back-reflected into the interferometer, we were able to simulate a parasitic interferences in any quadrature. The entangled light was generated from two squeezed modes following the scheme in [23]. One mode of the entangled state was introduced into the interferometer dark port via a polarizing beam-splitter (PBS) and a Faraday rotator. The output field was transmitted by the PBS and was overlapped at a 50 : 50 beam-splitter with the other entangled mode. Both beam-splitter outputs were simultaneously detected via balanced homodyne detection (BHD). A more detailed explanation of the experi-

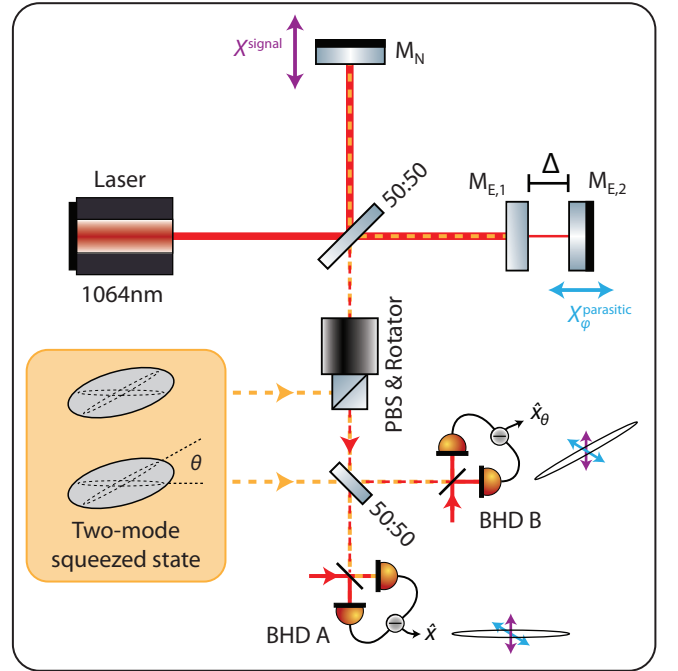


FIG. 2. Schematic setup for the experimental demonstration of quantum dense metrology. Two signals $X^{\text{signal}}(t)$ and $X_\phi^{\text{parasitic}}(t)$ are generated in a Michelson interferometer by modulating the PZT mounted mirrors M_N and $M_{E,2}$, respectively. $X^{\text{signal}}(t)$ is a pure phase modulation, while $X_\phi^{\text{parasitic}}(t)$ can be rotated into an arbitrary quadrature by adjusting Δ , which is the microscopic spacing between the east mirrors. A Faraday rotator couples one part of the entangled state into the interferometer. The other part is overlapped with the signal leaving the interferometer. The two resulting beams are simultaneously detected with balanced homodyne detectors, BHD A & B, measuring quadratures \hat{x} and $\hat{x}_{\theta \neq 0}$, respectively $\hat{p} = \hat{x}_{\theta = \pi/2}$. Revealing a parasitic interference requires neither the knowledge of ϕ nor matching θ to ϕ .

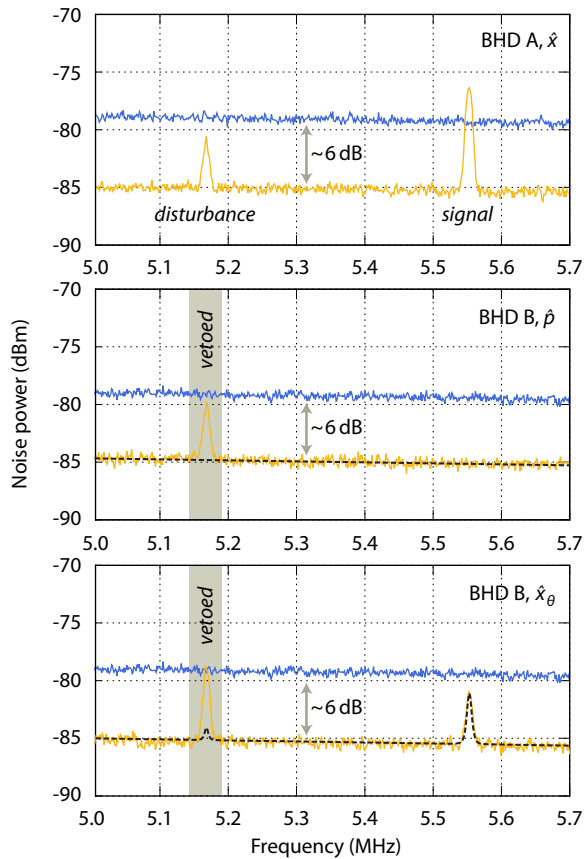


FIG. 3. Experimental demonstration of quantum-dense metrology for the identification of parasitic interferences. The orange traces show the detected signal variances at BHD A, $\Delta^2 \hat{x}$ (top panel) and BHD B, $\Delta^2 \hat{p}$ (middle) and $\Delta^2 \hat{x}_\theta$ (bottom). Parasitic signals are revealed due to their unexpected scaling in the lower two panels. The calculated scalings of science signals are shown in the dashed black curves. In the bottom panel, the angle θ was tuned so that part of the signal was recovered. The blue traces show the vacuum noise power of our BHDs, which are slightly sloped due to the decreasing transfer function of the homodyne detectors. All traces were recorded with RBW 10 kHz, VBW 100 Hz and averaged three times.

mental setup is given in the methods.

The results of our experiment are presented in Fig. 3. The first panel shows the power spectrum of the amplitude quadrature measurement of BHD A, which generally provides the highest signal-to-noise-ratio for the interferometric science signal (here at 5.55 MHz, orange trace). Due to the injected entangled light the readout noise is reduced to 6 dB below the vacuum noise (blue trace). BHD A also clearly detects a second (parasitic) signal at 5.17 MHz. Only by simultaneously looking at \hat{p} , as it is done with BHD B (second panel), the parasitic nature of the lower frequency signal is revealed: while the phase signal at 5.55 MHz vanishes as expected, the signal at 5.17 MHz does not vanish but actually increases in size.

This information is sufficient to reveal the parasitic nature of the lower frequency signal. Also the second BHD shows readout noise roughly 6 dB below vacuum noise. Simultaneous squeezing in two orthogonal quadratures is unique to our quantum-dense readout scheme.

In the third panel of Fig. 3, we used an improved strategy to reveal the parasitic signal. We detuned the angle θ between the original squeezing ellipses away from 90° . This way it is possible to retain at least part of the science signal in BHD B, while still having insight into the orthogonal quadrature. Since it can be exactly calculated how a phase signal measured at BHD A is projected into the \hat{x}_θ quadrature, any discrepancy reveals a parasitic signal. The dashed black lines in the second and third panels show the projected noise power, assuming that the first panel contains only phase signals. While the signal at 5.55 MHz perfectly matches the expectation, the disturbance at 5.17 MHz clearly does not. The advantage of the measurement in third panel is that, together with the first panel, the overall signal-to-noise-ratio of the science signal is improved. Changing θ allows for a smooth tuning between full signal coverage ($\theta = 0$), but no information about the conjugate observable; and maximum information about the disturbances in the full phase space ($\theta = \pi/2$), but loss of half the science signal power.

Conclusions — Interference is the basis for many high precision measurements and parasitic interferometer signals are a general problem that hampers the usefulness of nonclassical approaches. We have introduced and experimentally demonstrated the concept of quantum-dense metrology. QDM makes use of the fact that the scientific signal of an interferometer generally appears in a well-determined quadrature. A parasitic interference, however, appears in an arbitrary quadrature orientation. QDM can distinguish between scientific and parasitic signals with unlimited precision beyond the meter’s ground state uncertainty, and we proposed and demonstrated that this can be used to create a veto channel for parasitic signals. Our approach uses steady-state entanglement and therefore does not rely on any kind of conditioning or post-selection, which would result in a loss of measurement time. For the first time we propose two-mode squeezing for metrology that is generated with a non-orthogonal relative squeezing angle. Such entangled states allow the optimization of the signal-to-noise ratio when QDM is applied.

Beyond what we have demonstrated here, it should be even possible to subtract parasitic signals from the measurement data without subtracting science signals. For this, two assumptions have to be made. First, the parasitic signals have a quasi-stationary phase space orientation, second, the science signals have a temporal or spectral shape that is different from the parasitic signal. Then, quantum tomography at the second balanced homodyne detector (B) can be used to gather information

about the parasitic signal's phase space orientation and its projected quadrature components. Another idea is keeping the local oscillator phase fixed and introducing a fitting parameter that describes by which magnitude the parasitic signal is projected onto the conventional read-out quadrature of the interferometer. Fitting parameters are already used in data analysis based on matched filtering and signal templates [28]. In both scenarios, QDM allows for sub shot-noise measurements even if the apparatus without QDM is limited by parasitic interferences, i.e. is not quantum noise limited. QDM as proposed here does not help in the case of pure parasitic *phase* signals, which are caused by thermally excited fluctuations of mirror surfaces and radiation pressure forces. Instead, it is a valuable tool against all types of parasitic signals having a phase space orientation different from the phase quadrature. Our scheme can be applied to high-precision laser interferometers such as gravitational-wave observatories, where it has high potential in identifying parasitic signals due to photon scattering or hitherto unknown mechanisms. We thus envision that QDM will widen the application of quantum metrology in ongoing and future high precision measurements.

Acknowledgements — We acknowledge discussions with Tobias Eberle, Vitus Händchen and Harald Lück. This research has been financed by the Deutsche Forschungsgemeinschaft (SFB TR7, project C8), the EU FP-7 project Q-ESSENCE and supported by the Centre for Quantum Engineering and Space-Time Research (QUEST) and the IMPRS on Gravitational Wave Astronomy.

[1] V. Giovannetti, S. Lloyd, and L. Maccone, *Nature Photonics* **5**, 222 (2011).
 [2] R. Schnabel, N. Mavalvala, D. E. McClelland, and P. K. Lam, *Nature Communications* **1**, 121 (2010).
 [3] M. Xiao, L.-A. Wu, and H. Kimble, *Phys. Rev. Lett.* **59**, 278 (1987).
 [4] P. Grangier, R. Slusher, B. Yurke, and A. LaPorta, *Phys. Rev. Lett.* **59**, 2153 (1987).
 [5] D. Leibfried, M. D. Barrett, T. Schaetz, J. Britton, J. Chiaverini, W. M. Itano, J. D. Jost, C. Langer, and D. J. Wineland, *Science* **304**, 1476 (2004).
 [6] P. Cappelaro, J. Emerson, N. Boulant, C. Ramanathan, S. Lloyd, and D. Cory, *Phys. Rev. Lett.* **94** (2005), 10.1103/PhysRevLett.94.020502.
 [7] H. Vahlbruch, S. Chelkowski, B. Hage, A. Franzen, K. Danzmann, and R. Schnabel, *Physical Review Letters* **95**, 1 (2005).
 [8] I. Afek, O. Ambar, and Y. Silberberg, *Science* **328**, 879 (2010).
 [9] W. Wasilewski, K. Jensen, H. Krauter, J. J. Renema, M. V. Balabas, and E. S. Polzik, *Phys. Rev. Lett.* **104**, 1 (2010).
 [10] B. Lücke, M. Scherer, J. Kruse, L. Pezzé, F. Deuretzbacher, P. Hyllus, O. Topic, J. Peise, W. Ertmer, J. Arlt,

L. Santos, A. Smerzi, and C. Klempt, *Science* **334**, 773 (2011).
 [11] J. Abadie, B. P. Abbott, R. Abbott, T. D. Abbott, M. Abernathy, and et al., *Nature Physics* **7**, 962 (2011).
 [12] A. Abramovici, W. E. Althouse, R. W. Drever, Y. Gürsel, S. Kawamura, F. J. Raab, D. Shoemaker, L. Sievers, R. E. Spero, K. S. Thorne, R. E. Vogt, R. Weiss, S. E. Whitcomb, and M. E. Zucker, *Science* **256**, 325 (1992).
 [13] H. Vahlbruch, S. Chelkowski, K. Danzmann, and R. Schnabel, *New Journal of Physics* **9**, 371 (2007).
 [14] J.-Y. Vinet, V. Brisson, and S. Braccini, *Physical Review D* **54**, 1276 (1996).
 [15] J.-Y. Vinet, V. Brisson, S. Braccini, I. Ferrante, L. Pinard, F. Bondu, and E. Tournié, *Physical Review D* **56**, 6085 (1997).
 [16] D. J. Ottaway, P. Fritschel, and S. J. Waldman, *Optics Express* **20**, 8329 (2012).
 [17] S. Hild, S. Chelkowski, A. Freise, J. Franc, N. Morgado, R. Flaminio, and R. DeSalvo, *Classical and Quantum Gravity* **27**, 015003 (2010).
 [18] A. Einstein, B. Podolsky, and N. Rosen, *Physical Review* **47**, 777 (1935).
 [19] G. M. D'Ariano, P. Lo Presti, and M. G. A. Paris, *Phys. Rev. Lett.* **87**, 1 (2001).
 [20] C. H. Bennett and S. J. Wiesner, *Phys. Rev. Lett.* **69**, 2881 (1992).
 [21] S. L. Braunstein and H. J. Kimble, *Phys. Rev. A* **61**, 042302 (2000).
 [22] Z. Y. Ou, S. F. Pereira, H. J. Kimble, and K. C. Peng, *Phys. Rev. Lett.* **68**, 3663 (1992).
 [23] A. Furusawa, J. L. Sørensen, S. L. Braunstein, C. A. Fuchs, H. J. Kimble, and E. S. Polzik, *Science* **282**, 706 (1998).
 [24] C. Silberhorn, P. Lam, O. Weiss, F. König, N. Korolkova, and G. Leuchs, *Physical Review Letters* **86**, 4267 (2001).
 [25] W. P. Bowen, R. Schnabel, and P. K. Lam, *Phys. Rev. Lett.* **90**, 4 (2003).
 [26] E. Arthurs and J. L. Kelly, *Bell Syst. Tech. J.* **44**, 725 (1965).
 [27] U. Leonhardt, *Measuring the quantum state of light* (Cambridge University Press, Cambridge, 1997).
 [28] B. Sathyaprakash and B. Schutz, *Living Rev. Relativity* **12** (2009).
 [29] S. Steinlechner, J. Bauchrowitz, T. Eberle, and R. Schnabel, "Strong EPR-steering with unconditional entangled states," (2011), arXiv:arXiv:1112.0461.
 [30] L. Schnupp, "Presentation at European Collaboration Meeting on Interferometric Detection of Gravitational Waves (Sorrent, Italy)," (1988).

SUPPLEMENTARY MATERIAL

Entangled-light generation. Our continuous-variable entangled light was generated by the source described in [29]. Two squeezed vacuum fields generated by type I parametric down-conversion in PPKTP were overlapped at a 50 : 50 beam splitter, thereby creating two-mode squeezed light. Both input fields carried a residual phase modulation from locking the optical parametric amplifiers. At the detection stage, this modulation was reused to align the homodyne detectors to the

squeezed quadratures. A single sideband modulation was imprinted on one of the squeezed fields by overlapping it with 80 MHz frequency-shifted light from an acousto-optical modulator. This sideband was used to lock the quadrature angle between the input squeezed states. It was also used to stabilize one mode of the entangled field to the Michelson interferometer by detecting the beat signal between the sideband and the interferometer input field behind one end-mirror.

Interferometer setup and control. The Michelson interferometer had an arm length of about 7.5 cm for the north arm. The east arm was about 1.5 cm shorter, which allowed us to use the so-called Schnupp modulation technique [30] for locking the interferometer to its dark fringe. Both end-mirrors were flat and had a power reflectivity of 99.98% (M_N) and 98% (M_{E1}). The north mirror was PZT mounted to create a phase modulation inside the interferometer. A second PZT mounted flat mirror M_{E2} with reflectivity of $\approx 20\%$ was placed a few millimeters behind M_{E1} , creating a (weakly coupled) Fabry-Pérot cavity. By tuning this cavity, the phase signal created by M_{E2} could be rotated into an arbitrary quadrature. A DC locking scheme detected the transmitted light and held the cavity on its operating point. Both PZTs were driven on a mechanical resonance to be able to create signals in the few megahertz regime where the detected squeezing was strongest.

Readout of orthogonal quadratures. Consider a continuous-wave laser beam with central frequency ω_0 . The quantum noise of this beam at the sideband frequencies $\pm\Omega$, measured with a resolution bandwidth of $\Delta\Omega$, can be described by time-dependent operators for the amplitude quadrature $\hat{a}_1(\Omega, \Delta\Omega, t)$ and the phase quadrature $\hat{a}_2(\Omega, \Delta\Omega, t)$. Here we restrict ourselves to a monochromatic signal at a fixed sideband frequency and therefore drop the explicit frequency dependency in the following treatment. The quadrature operators satisfy the commutation relation $[\hat{a}_1, \hat{a}_2] = i$ and are normalized such that for a (squeezed) minimum uncertainty state $\Delta^2\hat{a}_1 = \Delta^2\hat{a}_2 = e^{\mp 2r}/2$, where the minus sign in the exponent belongs to the amplitude quadrature and the plus sign to the phase quadrature. r is the squeezing parameter, therefore $r = 0$ corresponds to a vacuum state, while $r < 0$ and $r > 0$ correspond to phase and amplitude squeezed light, respectively.

A measurement adds (classical) amplitude and phase modulations $X(t)$, $P(t)$ to the laser beam. The output field can then be described by the field quadrature vector

$$\hat{\mathbf{m}} = \begin{pmatrix} \hat{x}(t) \\ \hat{p}(t) \end{pmatrix} = \begin{pmatrix} \hat{a}_1(t) + X(t) \\ \hat{a}_2(t) + P(t) \end{pmatrix}. \quad (4)$$

From the commutation relation we can infer the Heisenberg uncertainty relation for the shot noise, normalized to the signal,

$$\frac{\Delta^2\hat{x}(t)}{|X(t)|^2} \frac{\Delta^2\hat{p}(t)}{|P(t)|^2} \geq \frac{1}{4|X(t)|^2|P(t)|^2}. \quad (5)$$

This inequality limits the simultaneous measurability of the amplitude and phase quadrature modulations. A simple approach to actually measure both quadratures in an Arthurs-Kelly type experiment is to split the beam at a 50 : 50 beam splitter – which introduces the vacuum mode $\hat{\mathbf{v}}$ – and then simultaneously perform a homodyne detection at each output port. Measuring the amplitude quadrature $\hat{x}_{\text{sim}} = (\hat{x} + \hat{v}_1)/\sqrt{2}$ in one detector and the phase quadrature $\hat{p}_{\text{sim}} = (\hat{p} - \hat{v}_p)/\sqrt{2}$ in the other leads to

$$\frac{\Delta^2\hat{x}_{\text{sim}}(t)}{|X_{\text{sim}}(t)|^2} \frac{\Delta^2\hat{p}_{\text{sim}}(t)}{|P_{\text{sim}}(t)|^2} \geq \frac{1 + \cosh(2r)}{2|X(t)|^2|P(t)|^2}, \quad (6)$$

where $X_{\text{sim}}(t) = X(t)/\sqrt{2}$ and $P_{\text{sim}}(t) = P(t)/\sqrt{2}$, since also the signal is divided at the beam splitter. Equation (4) states that the achievable minimum uncertainty is indeed at least four times larger than the limit imposed by Eq. (3). Squeezing does not help in this measurement scenario and the best sensitivity is achieved with vacuum input, i.e. $r = 0$.

For QDM, consider two squeezed vacuum modes with squeezing parameters r_a and r_b , described by the quadrature vectors $\hat{\mathbf{a}}$ and $\hat{\mathbf{b}}$. For simplicity, we restrict ourselves to the case where beam $\hat{\mathbf{a}}$ is always squeezed in the amplitude quadrature and the other beam is rotated in the quadrature space by θ . After entangling these beams at a 50 : 50 beam splitter, one mode is used as the meter state $\hat{\mathbf{m}}$ which is modulated with the signals $X(t)$, $P(t)$ as above, while the other state $\hat{\mathbf{r}}$ is kept as a reference beam. These two modes are then recombined at another beam splitter, whose two output fields are sent to balanced homodyne detectors A and B measuring the quadrature fields

$$\hat{x}_{\text{sim}}^{\text{ent}} = \frac{1}{\sqrt{2}}(\hat{r}_1 - \hat{x}) = \hat{a}_1 - X_{\text{sim}}^{\text{ent}}(t), \quad (7)$$

and

$$\hat{x}_{\theta, \text{sim}}^{\text{ent}} = \frac{1}{\sqrt{2}}(\hat{r}_\theta + \hat{x}_\theta) = \hat{b}_\theta + X_{\theta, \text{sim}}^{\text{ent}}(t), \quad (8)$$

respectively. Here, $\hat{x}_\theta = \hat{x} \cos \theta + \hat{p} \sin \theta$, $X_\theta(t) = X(t) \cos \theta + P(t) \sin \theta$ and the signals are again scaled by $1/\sqrt{2}$ since they are equally divided between the two homodyne detectors. The corresponding uncertainty product reads

$$\frac{\Delta^2\hat{x}_{\text{sim}}^{\text{ent}}(t)}{|X(t)|^2/2} \frac{\Delta^2\hat{x}_{\theta, \text{sim}}^{\text{ent}}(t)}{|X_\theta(t)|^2/2} = \frac{e^{-2r_a}e^{-2r_b}}{|X(t)|^2|X_\theta(t)|^2}. \quad (9)$$

This uncertainty is not bounded from below, for $r_a, r_b \rightarrow \infty$. Thus we have shown that quantum-dense metrology, which is performed in relation to a reference beam, can in principle reach arbitrarily high signal-to-noise ratios.